J Nanopart Res (2015)17:315
DOI 10.1007/s11051-015-3111-5

RESEARCH PAPER

Timescale of silver nanoparticle transformation in neural cell cultures impacts measured cell response

Stephanie L. Hume · Ann N. Chiaramonti · Katherine P. Rice · Rani K. Schwindt · Robert I. MacCuspie · Kavita M. Jeerage

Received: 29 January 2015 / Accepted: 7 July 2015

Abstract Both serum protein concentration and ionic strength are important factors in nanoparticle transformation within cell culture environments. However, silver nanoparticles are not routinely tracked at their working concentration in the specific medium used for in vitro toxicology studies. Here we evaluated the transformation of electrostatically stabilized citrate nanoparticles (C-AgNPs) and sterically stabilized polyvinylpyrrolidone nanoparticles (PVP-AgNPs) in a low-serum ($\sim$ 0.2 mg/mL bovine serum albumin) culture medium, while measuring the response of rat cortex neural progenitor cells, which differentiate in this culture environment. After 24 h, silver nanoparticles at concentrations up to 10 μg/mL did not affect adenosine triphosphate levels, whereas silver ions decreased adenosine triphosphate levels at concentrations of 1.1 μg/mL or higher. After 240 h, both silver nanoparticles, as well as silver ion, unambiguously decreased adenosine triphosphate levels at concentrations of 1 and 1.1 μg/mL, respectively, suggesting particle dissolution. Particle transformation was investigated in 1:10 diluted, 1:2 diluted, or undiluted differentiation medium, all having an identical protein concentration, to separate the effect of serum protein stabilization from ionic strength destabilization. Transmission electron microscopy images indicated that particles in 1:10 medium were not surrounded by proteins, whereas particles became clustered within a non-crystalline protein matrix after 24 h in 1:2 medium and at 0 h in undiluted medium. Despite evidence for a protein corona, particles were rapidly destabilized by high ionic strength media. Polyvinylpyrrolidone increased the stability of singly dispersed particles compared to citrate ligands; however, differences were negligible after 4 h in 1:2 medium or after 1 h in undiluted medium. Thus low-serum culture environments do not provide sufficient colloidal stability for long-term toxicology studies with citrate- or polyvinylpyrrolidone-stabilized silver nanoparticles.

Ann N. Chiaramonti and Katherine P. Rice have contributed equally to this work.

Electronic supplementary material The online version of this article (doi:10.1007/s11051-015-3111-5) contains supplementary material, which is available to authorized users.

S. L. Hume · A. N. Chiaramonti · K. P. Rice · R. K. Schwindt · K. M. Jeerage (✉)
Applied Chemicals and Materials Division, National Institute of Standards and Technology (NIST), MS 647, 325 Broadway, Boulder, CO 80305, USA
e-mail: jeerage@boulder.nist.gov

R. I. MacCuspie
Materials Measurement Science Division, National Institute of Standards and Technology (NIST), 100 Bureau Drive, Gaithersburg, MD 20899, USA

Published online: 21 July 2015

Keywords Agglomeration · Bovine serum albumin · Citrate · Dissolution · Ionic strength · Polyvinylpyrrolidone · Metallic nanoparticles

Introduction

Due to the anti-microbial properties of metallic silver, silver nanoparticles are found in hundreds of consumer products, presenting numerous routes for human exposure. Silver nanoparticles in systemic circulation can reach the liver, kidney, spleen, and brain (Tang et al. 2009). When silver nanoparticles are inhaled, silver is detectable within the brain and also the olfactory bulb (Ji et al. 2007; Sung et al. 2009; Takenaka et al. 2001), providing an alternate route to the central nervous system (Oberdorster et al. 2009). Silver nanoparticle toxicity, like that of other metal nanoparticles, is likely to be mediated by oxidative stress (Nel et al. 2006), which has been reported to disrupt cytoskeletal proteins (Allani et al. 2004) and inhibit neurite outgrowth (Neely et al. 1999). In humans, the central nervous system has a long developmental period and the adult mammalian brain contains a percentage of stem cells which remains capable of differentiation into neurons and astrocytes (Reynolds and Weiss 1992). Therefore, in vitro studies with developmental models are important to understanding the overall toxicology of silver nanoparticles.

Studies with model neural cells showed dopamine depletion (Hussain et al. 2006) and gene expression changes consistent with oxidative stress (Wang et al. 2009) upon exposure to 15 nm silver nanoparticles. These effects were observed after 24 h with relatively high exposures (5–50 μg/mL). Exposure to 5 μg/mL polyvinylpyrrolidone-stabilized silver nanoparticles of similar diameter increased apoptosis after 24 h; an increase in dead cells was observed after 48 h (Hadrup et al. 2012), and dissolution of the particles was inferred. Only a limited number of studies have examined the toxicological effects of silver nanoparticles on primary neural cells. In cultures containing neurons and astrocytes, 20 and 40 nm peptide-coated silver nanoparticles induced the formation of reactive oxygen species after 1 h (Haase et al. 2012). For a consistent mass dose (10 μg/mL), 20 nm particles produced a greater effect than 40 nm particles, suggesting that surface area was an important factor. Other studies (Liu et al. 2009, 2011) identified detrimental effects on hippocampal neurons at similarly high (10 μg/mL) exposures, though it is unlikely that such high applied in vitro doses would reach the central nervous system in vivo (Oberdorster 2010). None of the studies described above involved developmental processes, which generally require long in vitro culture periods. By contrast, neural progenitor cells are an emerging model for in vitro toxicology studies (Breier et al. 2010) in which developmental processes such as proliferation (Buzanska et al. 2009; Moors et al. 2009), differentiation (Buzanska et al. 2009; Fritsche et al. 2005; Jeerage et al. 2012; Moors et al. 2009), and neurite outgrowth (Jeerage et al. 2012) can be evaluated. Exposure to 20 nm and 80 nm silver nanoparticles was recently reported to increase the fraction of proliferative and apoptotic cells after 2 weeks (Soderstjerna et al. 2013). For neurite outgrowth, we recently demonstrated that 10 days of in vitro development was required for sensitivity to a known neuroactive chemical, whereas 5 days were insufficient (Jeerage et al. 2012).

In vitro toxicology studies of silver nanoparticles are complicated by the well-known instability of silver nanoparticle suspensions (MacCuspie et al. 2013). It has been demonstrated that silver nanoparticles release ions in aqueous environments due to oxidative dissolution (Liu and Hurt 2010), which increases the toxicity of silver nanoparticle suspensions (Beer et al. 2012; Kittler et al. 2010a). During long-term storage, a limiting value of dissolved silver is reached, which depends on temperature and stabilizer (Kittler et al. 2010a) as well as particle size (Zhang et al. 2011). Interestingly, agglomeration does not significantly impact ion release, since much of the surface remains available for reaction (Liu and Hurt 2010). In biological solutions, ionic strength and serum proteins strongly influence silver nanoparticle stability. For nanoparticles stabilized by weakly bound citrate ligands, which provide electrostatic repulsion in water, $CaCl_2$ concentrations of 1 mmol/L or NaCl concentrations of 50 mmol/L induced charge screening and rapid agglomeration (MacCuspie 2011). Cell culture medium contains these salts at similar or higher concentrations; however, protein adsorption can promote stability by both steric and electrostatic repulsion. For example, the presence of approximately 20 mg/mL bovine serum albumin in cell culture

medium allowed rapid adsorption to citrate-stabilized gold and silver nanoparticles, providing stability for 2 days (Zook et al. 2011b). Bovine serum albumin was also the critical component that allowed silver nanoparticles to remain stable at physiological concentrations of sodium chloride (154 mmol/L) in synthetic lung fluid (MacCuspie et al. 2011). However, even when bovine serum albumin was allowed to adsorb particles prior to injection into the culture medium, minor formulation differences dramatically altered nanoparticle agglomeration over approximately 2 days (MacCuspie 2011). Adsorption of polyvinylpyrrolidone ligands, which provide steric repulsion in water, provides increased stability to silver nanoparticles in environmental solutions (Tejamaya et al. 2012) but have been less studied in biological solutions containing serum proteins. While many model cells are cultured in medium containing 10 % serum, differentiation medium for neural progenitor cells contains 1 % serum (Reynolds and Weiss 1996), which provides approximately 0.2 mg/mL bovine serum albumin. Considering the importance of ionic strength, serum proteins, and formulation on particle transformation, we cannot predict a priori which stabilization approach will be superior during a multiple-day culture period.

In this work, we examined the impact of silver nanoparticles stabilized by citrate ligands, silver nanoparticles stabilized by polyvinylpyrrolidone ligands, and silver ions alone on the metabolism of rat cortex neural progenitor cells. We screened a wide range of concentrations to determine exposures that unambiguously altered metabolism after 24 or 240 h. To interpret these results, we investigated the ability of nanoparticles to interfere with the luminescent metabolic assay, the transformation of silver nanoparticles in low-serum culture medium, and the timescale over which transformation occurred. Electron microscopy was employed to visualize formation of the protein corona and ultraviolet–visible spectroscopy was employed to indicate singly dispersed particles. Dilutions containing 10 or 50 % of the salt concentration, but the same protein concentration, were utilized to separate the effect of serum protein stabilization from ionic strength destabilization. Our results demonstrate that the timescale of silver nanoparticle transformation in the specific cell culture environment must be considered when interpreting in vitro toxicology results.

Materials and methods[1]

Silver nanoparticle synthesis and dispersion

Citrate-stabilized silver nanoparticles (C-AgNPs) of approximately 20 nm diameter were synthesized by reducing an aqueous solution of boiling silver nitrate in the presence of trisodium citrate with sodium borohydride (MacCuspie 2011). C-AgNPs were concentrated by stirred cell ultrafiltration through a 10,000 Da molecular weight cut-off regenerated cellulose filter. Based on previous studies, the reaction goes to more than 99 % of completion based on the mass of silver nitrate added. From the mass and final volume after concentration, the total silver in the stock suspension was 0.978 mg/mL (reported throughout this work as 1 mg/mL).

Polyvinylpyrrolidone-stabilized silver nanoparticles (PVP-AgNPs) were produced by adding 10 mg/mL PVP10 (10,000 g/mol average molecular weight, Sigma-Aldrich) to 1 mg/mL C-AgNPs (0.2 g polymer added to 20 mL stock suspension) and stirring overnight while covered. Nanoparticle stock suspensions were stored at 4 °C in the dark and used over the course of 6 weeks. Stock suspensions were periodically diluted for hydrodynamic diameter measurements to ensure that they remained stable.

Complete differentiation medium was prepared by combining basal medium with differentiation supplements containing serum. Solutions containing a 1:9 or a 1:1 ratio of basal medium and deionized water were combined with differentiation supplements to create solutions with 10 or 50 % of the salt concentration, but the same protein concentration as the differentiation medium was used for cell culture. These solutions are referred to as 1:10 medium and 1:2 medium, respectively. Stock nanoparticle suspensions were added to deionized water, 1:10 medium, 1:2 medium, or complete differentiation medium and mixed by gentle pipetting.

[1] Certain commercial equipment, instruments, or materials are identified in this document. Such identification does not imply recommendation or endorsement by the National Institute of Standards and Technology, nor does it imply that the products identified are necessarily the best available for the purpose.

Neural progenitor cell culture

Rat cortex neural stem/progenitor neurospheres isolated at embryonic day 18 were obtained from StemCell Technologies. Proliferation and differentiation media (Neurocult NS-A) were prepared according to the manufacturer's instructions. Neurospheres were resuspended in proliferation medium and passaged into a single cell suspension after 24 h. Proliferation medium was partially exchanged after 48 h; cells were seeded in differentiation medium after an additional 48 h at a density of 1.25×10^5 cells/cm^2, equivalent to 4×10^4 cells/well. Culture surfaces within opaque white 96-well assay plates (0.32 cm^2, Corning) had been previously incubated with 15 μg/mL poly-L-ornithine (Sigma-Aldrich) to promote cell attachment.

Cells were allowed to attach for 4 h prior to chemical or nanoparticle exposure. Silver nitrate (Alfa Aesar) was dissolved in complete medium and filtered (0.22 μm polyethersulfone membrane, Corning). Silver nitrate stock solutions were added 1:4 to wells, for final silver concentrations of 0.011, 0.032, 0.11, 0.32, 1.1, or 3.2 μg/mL. Nanoparticle suspensions in complete differentiation medium were mixed from either C-AgNP or PVP-AgNP stock suspensions, and immediately added 1:4 to wells to obtain final silver concentrations of 0.1, 0.3, 1, 3, and 10 μg/mL.

Adenosine triphosphate (ATP) evaluation

The CellTiter-Glo Luminescent Cell Viability Assay (Promega) was used after 1 day or 10 days in culture. Luminescence intensity was measured with a Synergy HT Multimode Plate Reader (Biotek) and was background-corrected. The emitted light is centered at 560 nm but is broad in spectrum, so agglomerated silver nanoparticles might absorb or scatter some of the signal. Nanoparticle interference was therefore evaluated by measuring standard curves (Supplementary Information, Fig. A.1 and Fig. A.2). ATP stock solution (10 mmol/L) was added to complete differentiation medium to yield 0.075, 0.75, 1.5, and 2.25 μmol/L for the standard curves. Freshly mixed C-AgNP or PVP-AgNP suspensions were added (final silver concentrations were 0.3, 1, 3, or 10 μg/mL); 3.2 μg/mL Ag^+ was added to evaluate silver ion interference.

All statistical analysis was performed with InStat (GraphPad Software). Each well was considered an individual sample and mean values are reported plus or minus standard error of the mean (S.E.M.). Results from individual cultures were normalized by controls from that culture and then combined with normalized values from other cultures. Means were compared by one-way analysis of variance (ANOVA), with $p < 0.05$ considered significant. Each pair of means was then evaluated by Dunnett's post-test to determine whether cultures were significantly different from controls.

Dynamic light scattering (DLS)

Silver nanoparticles were dispersed in deionized water or complete differentiation medium (10 μg/mL) and added to a low-volume quartz cuvette (ZEN2112) for size measurements with a Zetasizer Nano (Malvern). This instrument employs a helium–neon (633 nm) laser and measures the scattered light at 173° (backscatter). Measurements were performed at 20 °C. Intensity size distributions were converted to volume size distributions by the software. Suspensions were stored in a cell culture incubator (37 °C, 5 % CO_2) and gently pipetted ten times before each measurement.

Ultraviolet–Visible spectroscopy

Silver nanoparticles were dispersed in deionized water, 1:2 medium, or complete differentiation medium (10 μg/mL). Spectra are reported as the average of two measurements made from 2 μL aliquots with a NanoDrop 2000 spectrophotometer (Thermo Scientific). Suspensions were stored in a cell culture incubator (37 °C, 5 % CO_2) and gently pipetted ten times before each measurement.

Electron microscopy

Silver nanoparticles were dispersed in deionized water, 1:10 medium, 1:2 medium, or complete differentiation medium (10 μg/mL). At each timepoint, 20 μL was drop cast onto an ultrathin (less than 3 nm) carbon membrane on a holey carbon-coated copper support grid. Samples prepared with 1:10 medium or 1:2 medium were gently swished in deionized water for 15 s and then air-dried overnight; samples prepared with complete medium were air-dried overnight. Transmission electron microscopy

(TEM) was performed in a LaB_6 instrument operated at 200 kV. Scanning electron microscopy (SEM) employed a field-emission instrument operated at 10 kV. SEM images with TEM-like contrast were acquired using a STEM conversion-type holder. The electron beam was scanned over the surface of the sample, and any electrons transmitted through the sample struck a gold-coated mirror reflector located below the specimen. The transmitted electrons that struck the gold were converted into secondary electrons, which were then detected using the normal in-chamber Everhart–Thornley secondary electron detector. There was a small contribution to the image from normal secondary electron generation, that is, secondary electrons generated in the sample and detected directly.

Results and discussion

Citrate ligands are commonly employed in silver nanoparticle synthesis. Citrate stabilizes silver nanoparticles electrostatically, via charge repulsion. By contrast, polyvinylpyrrolidone is a hydrophilic polymer adsorbed to the metal core, providing steric stabilization. DLS results indicate that the citrate-stabilized AgNPs and the polyvinylpyrrolidone-stabilized AgNPs utilized in this work have similar hydrodynamic diameters. When diluted in deionized water, a bi-modal intensity size distribution was observed for both C-AgNPs and PVP-AgNPs (Fig. 1a). Intensity size distributions are dominated by large particles because the Rayleigh scattering intensity is proportional to the sixth power of the particle radius. The volume size distribution, derived from the intensity size distribution and more directly comparable to mass-based dose metrics, is monomodal for both C-AgNPs and PVP-AgNPs (Fig. 1b), with the peak centered at 19 and 25 nm, respectively. Because the silver cores came from the same synthesis, the observed difference in hydrodynamic diameter (6 nm) is attributed to the adsorbed polymer. For particles stored in water at 4 °C, DLS measurements similar to Fig. 1 were obtained over 6 weeks. Approximately 6 months after synthesis, a small amount of agglomeration was noted for PVP-AgNPs (20 % larger) whereas C-AgNPs remained at their original distribution.

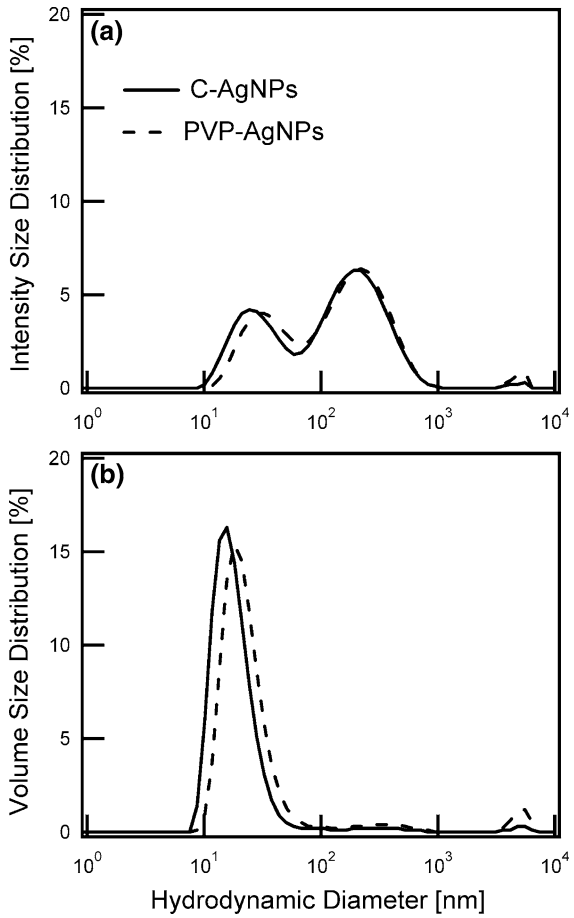

Fig. 1 DLS intensity size distribution (**a**) and volume size distribution (**b**) of 10 μg/mL C-AgNPs and 10 μg/mL PVP-AgNPs dispersed in deionized water

Adenosine triphosphate (ATP) levels indicate a delayed metabolic response to silver nanoparticles compared to silver ions

Culture-level metabolism was evaluated following exposure to a wide range of silver ion and nanoparticle concentrations via the enzymatic conversion of beetle luciferin to oxyluciferin, which is proportional to adenosine triphosphate (ATP) levels. This assay is particularly sensitive to low cell numbers (Petty et al. 1995), which were employed here. Cultures exposed to silver ions had a classic dose–response relationship after 1 day (Fig. 2), with no change in ATP levels, relative to control levels, for 0.32 μg/mL Ag^+ or lower. Exposure to 1.1 μg/mL Ag^+ decreased ATP levels by approximately 25 %, and exposure to 3.2 μg/

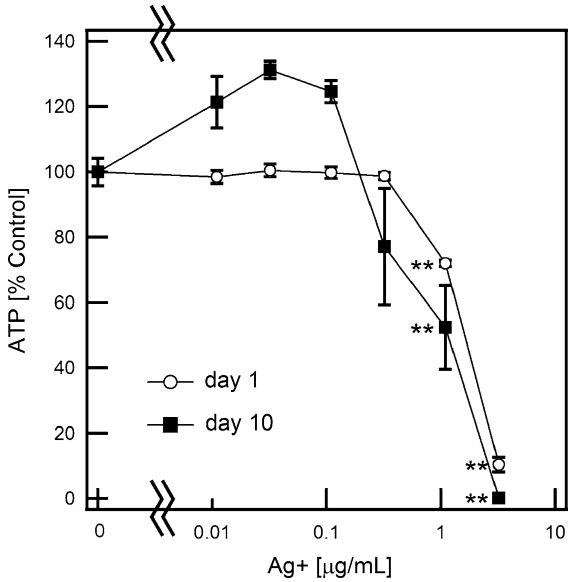

Fig. 2 ATP levels in cultures exposed to Ag^+ until evaluation after 1 day or 10 days. Reported values are based on ten wells from two independent cultures. *Stars* indicate significant differences from controls in post-test comparisons (**$p < 0.01$)

mL Ag^+ decreased ATP levels by approximately 90 %. For these concentrations, the response after 10 days was greater (50 % decrease for 1.1 μg/mL Ag^+, 100 % decrease for 3.2 μg/mL Ag^+) but did not change the threshold concentration (1.1 μg/mL Ag^+). However, it is noteworthy that cultures exposed to 0.32 μg/mL Ag^+ had an unusually large variation in response. Interestingly, sub-lethal Ag^+ exposure seemed to stimulate the cultures after 10 days. Such low-dose stimulation combined with high-dose inhibition, resulting in a biphasic curve, has been described as a common dose–response relationship that is often difficult to demonstrate with statistical significance (Calabrese and Baldwin 2003). This is because ANOVA analysis is dominated by the main trend, which is the decrease at high doses. When only the low-dose regime (0.011 to 0.11 μg/mL Ag^+) is considered, the p value is less than 0.001.

Cultures exposed to C-AgNPs (Fig. 3a) or PVP-AgNPs (Fig. 3b) had no change in ATP levels, relative to control levels, after 1 day. However, after 10 days, nanoparticle exposure at 1 μg/mL decreased ATP levels by nearly 50 % for C-AgNPs and nearly 70 % for PVP-AgNPs. These values are not significantly different from each other. Exposure to either

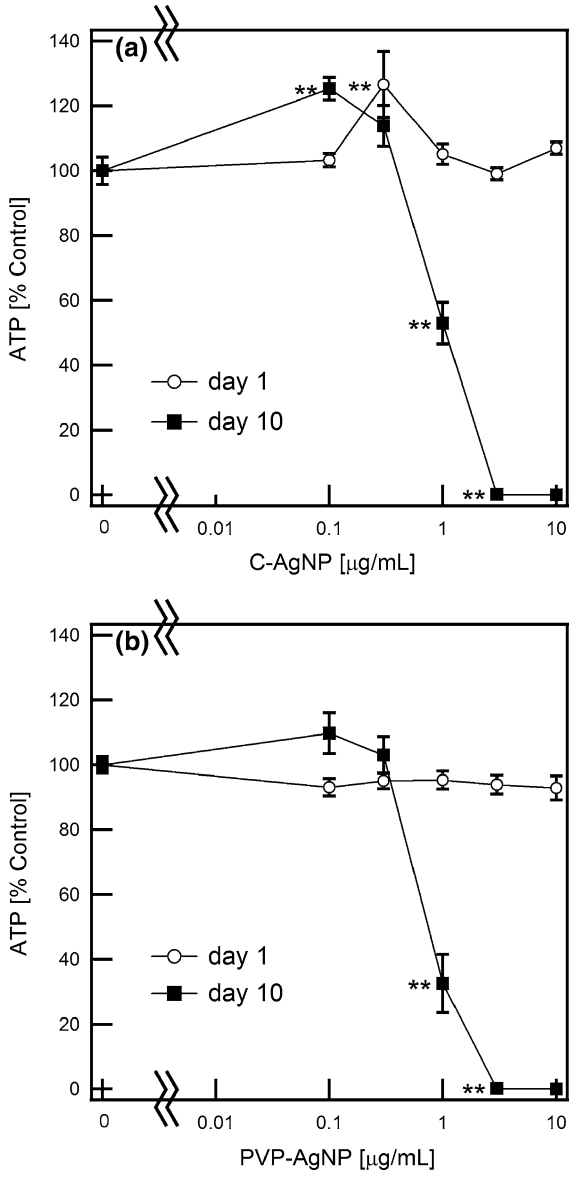

Fig. 3 ATP levels in cultures exposed to C-AgNPs (**a**) or PVP-AgNPs (**b**) until evaluation after 1 day or 10 days. Reported values are based on ten wells from two independent cultures, except for the 0.1 μg/mL condition (C-AgNPs, but not PVP-AgNPs), which was evaluated with five wells from one culture. *Stars* indicate significant differences from controls in post-test comparisons (**$p < 0.01$)

nanoparticle at 3 μg/mL or higher decreased ATP levels by essentially 100 %, which likely indicated death of all cells in culture. For concentrations of 1 μg/mL or higher, values in Fig. 3 were adjusted to account for silver nanoparticle interference with the luminescence measurement (Supplementary Information,

Fig. A.1). Note that values in Fig. 2 were not adjusted, as silver ions (3.2 μg/mL) did not interfere with the luminescence measurement (Supplementary Information, Fig. A.2).

The threshold nanoparticle dose identified here (1 μg/mL) is lower than the smallest dose examined in most in vitro studies of silver nanoparticles and model neural cells (Hadrup et al. 2012; Hussain et al. 2006; Wang et al. 2009) or primary neural cells (Haase et al. 2012; Liu et al. 2009, 2011). However, it is higher than the dose identified in studies of the growth characteristics of neural progenitor cells (Soderstjerna et al. 2013), suggesting that neural progenitor cells are less susceptible to silver ions during differentiation. The correspondence between the threshold dose identified for silver ions (1.1 μg/mL) and both silver nanoparticles (1 μg/mL) suggests that dissolution of the nanoparticles must be considered. However, dissolution cannot be immediate, given that culture-level metabolism was significantly reduced by silver ions, but not nanoparticles, after 24 h. In the studies which follow, particles were investigated in 1:10 diluted, 1:2 diluted, or undiluted (complete) differentiation medium, having an identical protein concentration, to separate the effect of serum protein stabilization from ionic strength destabilization.

Ionic strength affects protein corona formation at 37 °C

We employed TEM images of samples prepared at 0 and 24 h, a timeframe which should illustrate the most dramatic changes, to probe the formation of a protein corona. TEM images are typically employed to determine particle size distribution, since the drying process tends to promote agglomeration. Here we assume that drying-induced distortions operate equally on all samples, allowing us to visualize changes as a function of ionic strength or time. TEM images of C-AgNPs dispersed in 1:10 medium appeared similar to particles dispersed in deionized water, with individual, evenly dispersed particles which did not change in appearance after 24 h of incubation (Fig. 4a). TEM images of C-AgNPs dispersed in 1:2 medium also showed individual, evenly dispersed particles at 0 h (Fig. 4b). However, after 24 h of incubation, particles were located within a non-crystalline matrix (as determined by focused-probe electron diffraction) which had not been observed at 0 h. Since the matrix was not crystalline salt, it was likely composed of serum proteins. Particles were rarely observed outside the matrix, based on examining multiple regions of the grid. Because the serum protein concentration was constant, these imaging results suggest that higher-salt formulations induced the clustering of particles within a protein matrix.

TEM images of PVP-AgNPs in complete medium indicated that clusters of particles were located within a non-crystalline protein matrix at 0 h (Fig. 4c). Transmission-mode SEM images of PVP-AgNPs in complete medium (Fig. 5) indicated that silver nanoparticle clusters were found within and without the non-crystalline protein matrix. In this image, non-crystalline matrix regions without apparent nanoparticle clusters also showed appreciable absorption, similar to silver nanoparticles. Because the support films (the carbon blanket film and the holey carbon support film) are nearly perfectly flat and of uniform thickness over the regions observed, the contrast in the image arose primarily from differences in atomic number, indicating that the scattering was from an element that is heavy relative to the carbon background. Their high contrast suggests a high concentration of silver ions, known to associate with proteins (Kittler et al. 2010b; Liu et al. 2012), within these regions.

Ionic strength affects timescale of transformation at 37 °C

Silver nanoparticles of 20 nm are expected to have an attenuance (absorbance plus scattering of ultraviolet–visible light) maximum around 400 nm. C-AgNPs and PVP-AgNPs in deionized water had attenuance peaks centered at approximately 390 and 395 nm, respectively. Freshly dispersed suspensions made from silver nanoparticle stocks (1 mg/mL) stored in the refrigerator (4 °C in the dark) had consistent attenuance, as expected from other studies (Liu and Hurt 2010). When 10 μg/mL suspensions in deionized water were stored under cell culture conditions (37 °C in the dark, 5 % CO_2), they slowly dissolved (Supplementary Information, Fig. A.3). Since there was no evidence for nanoparticle agglomeration, which would be indicated by red-shifted peaks, the area under the attenuance curve (Zook et al. 2011a) was used to compare dissolution of the silver nanoparticles. This

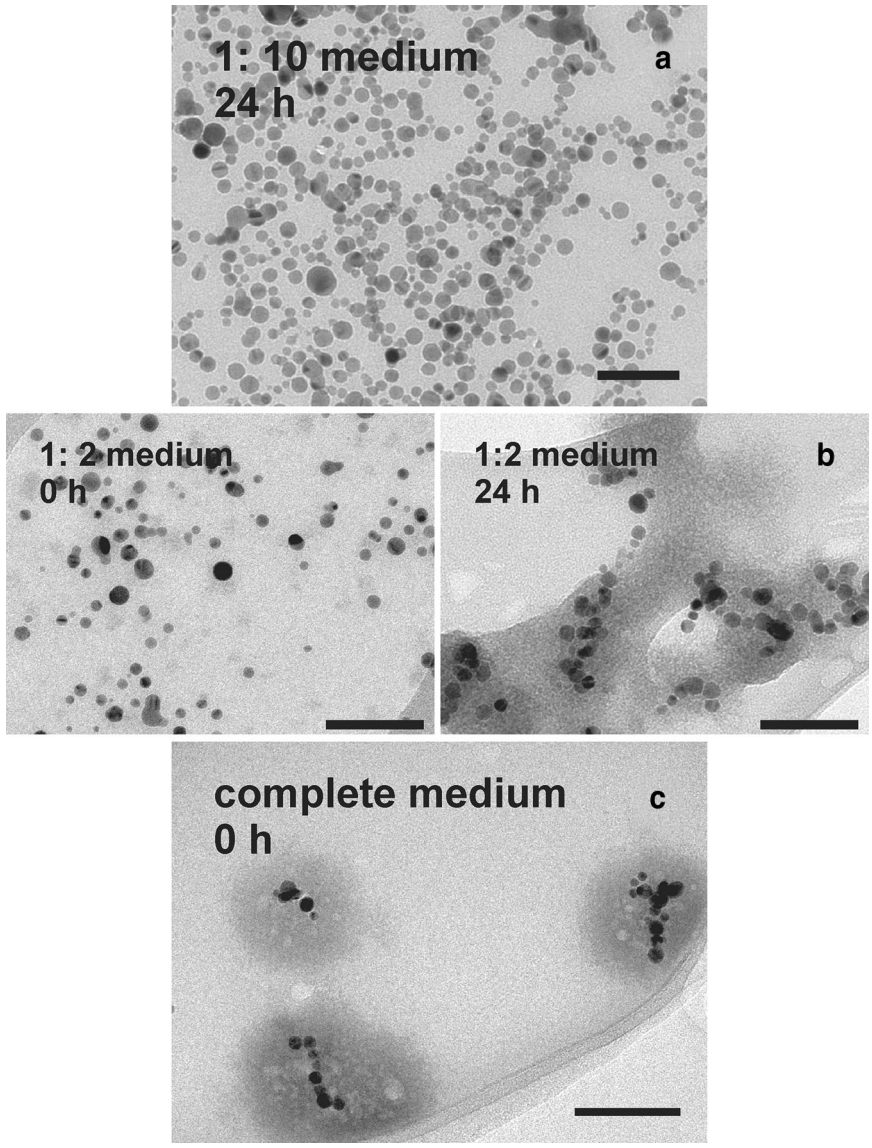

Fig. 4 Bright field TEM images of **a** C-AgNPs dispersed in 1:10 medium after 1 day of incubation (24 h), **b** C-AgNPs dispersed in 1:2 medium, immediately after preparation (0 h) and after 1 day of incubation (24 h), and **c** PVP-AgNPs dispersed in complete differentiation medium, immediately after preparation (0 h). *Scale bars* are 100 nm

method indicated that dissolution was 16 % after 24 h and 37 % after 240 h for C-AgNP suspensions. For PVP-AgNP suspensions, dissolution was 7 % after 24 h and 43 % after 240 h. In summary, similar dissolution rates were observed for C-AgNPs and PVP-AgNPs in deionized water.

Complete differentiation medium contains 1.8 mmol/L of Ca^{2+} and Mg^{2+} as well as 125 mmol/L of NaCl and KCl (Reynolds and Weiss 1996); these concentrations are sufficient to induce rapid agglomeration of citrate-stabilized particles in the absence of steric stabilization by bovine serum albumin (MacCuspie 2011). Freshly dispersed C-AgNPs were too polydisperse for cumulant analysis; after 24 h, the Z-average size was greater than 500 nm and values from 500 nm to 600 nm were measured at subsequent timepoints (data not shown). Freshly dispersed PVP-AgNPs had a Z-average size of 110 nm, but after 24 h, the Z-average size was greater than 400 nm and values from 500 to 800 nm were measured at subsequent timepoints (data not shown). To focus on unagglomerated particles, if any, attenuance spectra were measured with additional timepoints at 1 h and 4 h.

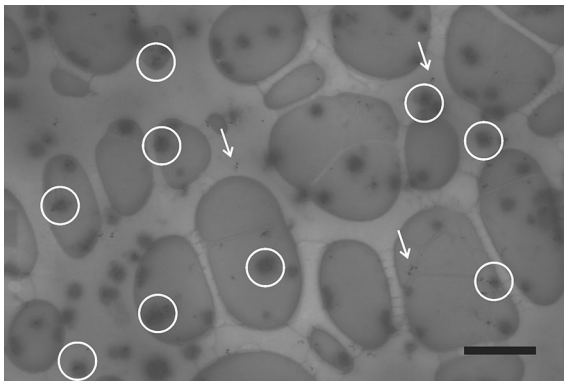

Fig. 5 Transmission-mode SEM image of PVP-AgNPs dispersed in complete differentiation medium (0 h) displaying primarily TEM-like contrast. Silver nanoparticles (*arrows*) and silver nanoparticles within a non-crystalline protein matrix (*circles*) are indicated; however, nanoparticles cannot be discerned within every non-crystalline matrix. The darkest contrast in the image arises primarily from atomic number, indicating that these regions contain an element that is heavy relative to carbon. Note that the holey carbon support film appears lighter than the carbon blanket film due to the small contribution to the image from secondary electrons generated in the sample and detected directly. *Scale bar* is 500 nm

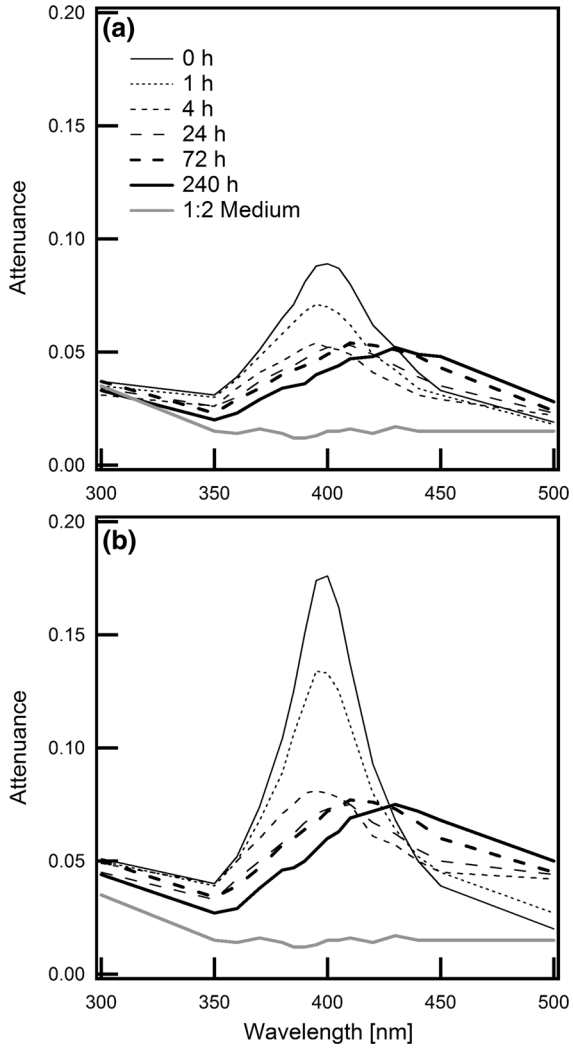

Fig. 6 UV–Vis spectra for 10 μg/mL C-AgNPs (**a**) and 10 μg/mL PVP-AgNPs (**b**) dispersed in 1:2 medium. Suspensions were incubated at 37 °C/5 % CO_2 between measurements. UV–Vis spectrum due to 1:2 medium is shown for reference

Immediately following dispersion in 1:2 medium, C-AgNPs (Fig. 6a) had an attenuance of approximately half of that observed in water, as well as a broader peak, whereas PVP-AgNPs (Fig. 6b) had an attenuance resembling that observed in water, reflecting the increased stability provided by the adsorbed polymer. Baseline measurements indicated little attenuance due to the presence of media alone. Over time, attenuance decreased slightly for C-AgNPs and rapidly for PVP-AgNPs and their respective peaks were similar in magnitude after 4 h. After 24 h, peaks for both particles had broadened considerably and red-shifted. This trend continued over time and after 240 h, peaks were centered at approximately 430 nm for both C-AgNPs and PVP-AgNPs, indicating that suspended agglomerates were formed during this time period.

Immediately following dispersion in complete differentiation medium, C-AgNPs had an attenuance of approximately one-fourth of that observed in water (Fig. 7a), whereas PVP-AgNPs again had an attenuance resembling that observed in water (Fig. 7b). However, the spectrum for PVP-AgNPs changed dramatically within the first hour, becoming similar to the spectrum for freshly dispersed C-AgNPs. For both particles, the diminished peak indicating unagglomerated particles measured at 0 h (C-AgNPs) or 1 h (PVP-AgNPs) red-shifted during the next 24 h, again indicating that suspended agglomerates were formed. Because the serum protein concentration was constant, these results show that higher-salt formulations shortened the timescale of transformation. Although high concentrations of bovine serum albumin (approximately 20 mg/mL) rapidly adsorbed to and stabilized C-AgNPs in other studies (Zook et al. 2011b), the low concentration of bovine serum albumin here (approximately 0.2 mg/mL) did not

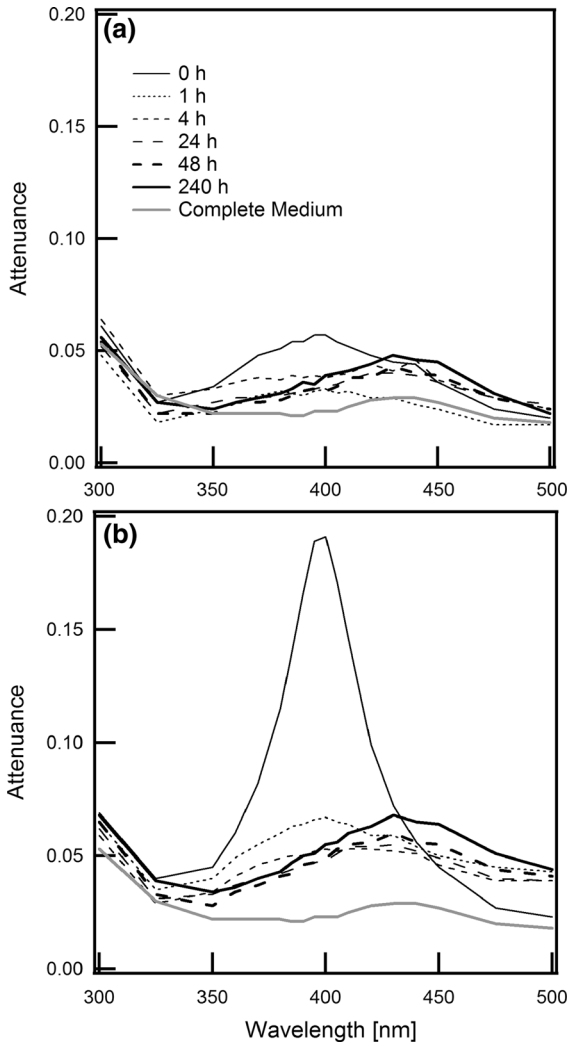

Fig. 7 UV–Vis spectra for 10 μg/mL C-AgNPs (**a**) and 10 μg/mL PVP-AgNPs (**b**) dispersed in complete medium. Suspensions were incubated at 37 °C/5 % CO_2 between measurements. UV–Vis spectrum due to complete medium is shown for reference

stabilize C-AgNPs at their original dimensions. It was recently reported that the addition of 10 mg/mL PVP to 1 mg/mL C-AgNPs (nominally identical to those employed here) was insufficient to stabilize the resulting PVP-AgNPs through lyophilization and reconstitution (MacCuspie et al. 2013). We conclude here that a low density of adsorbed polymer did not stabilize PVP-AgNPs at their original dimensions for time periods relevant to in vitro neurodevelopmental assays.

Conclusions

Overall, this work demonstrated that a low density of adsorbed polyvinylpyrrolidone did not improve silver nanoparticle stability compared to citrate ligands, for timescales relevant to neural progenitor cell development, in a low-serum culture environment. When dispersed in complete differentiation medium, a large fraction of the silver nanoparticles formed agglomerates within the first hour. Nanoparticle clusters were visualized within a non-crystalline protein matrix and contributed to the decrease in luminescent intensity observed for freshly dispersed (0 h) and aged (24 h) particles. The small fraction of particles which remained at their original dimensions after 1 h slowly agglomerated during further incubation. Since large agglomerates are less likely to interact with cells, slow release of silver ions is the dominant phenomenon in this culture environment. Therefore, the culture-level metabolism of developing neural progenitor cells did not decrease after 24 h exposure to silver nanoparticles at concentrations up to 10 μg/mL, but did decrease after 240 h exposure to 1 μg/mL silver nanoparticle suspensions. Thus low-serum culture environments do not provide sufficient colloidal stability for long-term in vitro toxicology studies with citrate or low-density polyvinylpyrrolidone-stabilized silver nanoparticles. Instead, the timescale over which nanoparticle transformation occurs must be simultaneously analyzed with the measured cell response, throughout the duration of in vitro toxicology studies.

Acknowledgments Stephanie L. Hume was supported by a National Research Council (NRC) postdoctoral fellowship through the American Recovery and Reinvestment Act. We thank Dr. Aric W. Sanders (Quantum Electronics and Photonics Division, Physical Measurement Laboratory, NIST Boulder) for his assistance with transmission-mode imaging.

References

Allani PK, Sum T, Bhansali SG, Mukherjee SK, Sonee M (2004) A comparative study of the effect of oxidative stress on the cytoskeleton in human cortical neurons. Toxicol Appl Pharmacol 196:29–36

Beer C, Foldbjerg R, Hayashi Y, Sutherland DS, Autrup H (2012) Toxicity of silver nanoparticles-nanoparticle or silver ion? Toxicol Lett 208:286–292

Breier J, Gassmann K, Kayser R, Stegeman H, De Groot D, Fritsche E, Shafer T (2010) Neural progenitor cells as models for high-throughput screens of developmental neurotoxicity: state of the science. Neurotoxicol Teratol 32:4–15

Buzanska L, Sypecka J, Nerini-Molteni S, Compagnoni A, Hogberg HT, del Torchio R, Domanska-Janik K, Zimmer J, Coecke S (2009) A human stem cell-based model for identifying adverse effects of organic and inorganic chemicals on the developing nervous system. Stem Cells 27:2591–2601

Calabrese EJ, Baldwin LA (2003) Hormesis: the dose-response revolution. Annu Rev Pharmacol Toxicol 43:175–197

Fritsche E, Cline JE, Nguyen NH, Scanlan TS, Abel J (2005) Polychlorinated biphenyls disturb differentiation of normal human neural progenitor cells: clue for involvement of thyroid hormone receptors. Environ Health Perspect 113:871–876

Haase A, Rott S, Mantion A, Graf P, Plendl J, Thunemann AF, Meier WP, Taubert A, Luch A, Reiser G (2012) Effects of silver nanoparticles on primary mixed neural cell cultures: uptake, oxidative stress and acute calcium responses. Toxicol Sci 126:457–468

Hadrup N, Loeschner K, Mortensen A, Sharma AK, Qvortrup K, Larsen EH, Lam HR (2012) The similar neurotoxic effects of nanoparticulate and ionic silver in vivo and in vitro. Neurotoxicology 33:416–433

Hussain SM, Javorina AK, Schrand AM, Duhart HM, Ali SF, Schlager JJ (2006) The interaction of manganese nanoparticles with PC12 cells induces dopamine depletion. Toxicol Sci 92:456–463

Jeerage KM, Oreskovic TL, Hume SL (2012) Neurite outgrowth and differentiation of rat cortex progenitor cells are sensitive to lithium chloride at non-cytotoxic exposures. Neurotoxicology 33:1170–1179

Ji JH, Jung JH, Kim SS, Yoon JU, Park JD, Choi BS, Chung YH, Kwon IH, Jeong J, Han BS, Shin JH, Sung JH, Song KS, Yu IJ (2007) Twenty-eight-day inhalation toxicity study of silver nanoparticles in Sprague-Dawley rats. Inhal Toxicol 19:857–871

Kittler S, Greulich C, Diendorf J, Koller M, Epple M (2010a) Toxicity of silver nanoparticles increases during storage because of slow dissolution under release of silver ions. Chem Mater 22:4548–4554

Kittler S, Greulich C, Gebauer JS, Diendorf J, Treuel L, Ruiz L, Gonzalez-Calbet JM, Vallet-Regi M, Zellner R, Koller M, Epple M (2010b) The influence of proteins on the dispersability and cell-biological activity of silver nanoparticles. J Mater Chem 20:512–518

Liu J, Hurt RH (2010) Ion release kinetics and particle persistence in aqueous nano-silver colloids. Environ Sci Technol 44:2169–2175

Liu ZW, Ren GG, Zhang T, Yang Z (2009) Action potential changes associated with the inhibitory effects on voltage-gated sodium current of hippocampal CA1 neurons by silver nanoparticles. Toxicology 264:179–184

Liu ZW, Ren GG, Zhang T, Yang Z (2011) The inhibitory effects of nano-Ag on voltage-gated potassium currents of hippocampal CA1 neurons. Environ Toxicol Pharmacol 26:552–558

Liu J, Wang ZL, Liu FD, Kane AB, Hurt RH (2012) Chemical transformations of nanosilver in biological environments. ACS Nano 6:9887–9899

MacCuspie RI (2011) Colloidal stability of silver nanoparticles in biologically relevant conditions. J Nanopart Res 13:2893–2908

MacCuspie RI, Allen AJ, Hackley VA (2011) Dispersion stabilization of silver nanoparticles in synthetic lung fluid studied under in situ conditions. Nanotoxicology 5:140–156

MacCuspie RI, Allen AJ, Martin MN, Hackley VA (2013) Just add water: reproducible singly dispersed silver nanoparticle suspensions on-demand. J Nanopart Res 15:1760

Moors M, Rockel TD, Abel J, Cline JE, Gassman K, Schreiber T, Schuwald J, Weinmann N, Fritsche E (2009) Human neurospheres as three-dimensional cellular systems for developmental neurotoxicity testing. Environ Health Perspect 117:1131–1138

Neely MD, Sidell KR, Graham DG, Montine TJ (1999) The lipid peroxidation product 4-hydroxynonenal inhibits neurite outgrowth, disrupts neuronal microtubules, and modifies cellular tubulin. J Neurochem 72:2323–2333

Nel AE, Xia T, Madler L, Li N (2006) Toxic potential of materials at the nanolevel. Science 311:622–627

Oberdorster G (2010) Safety assessment for nanotechnology and nanomedicine: concepts of nanotoxicology. J Intern Med 267:89–105

Oberdorster G, Elder A, Rinderknecht A (2009) Nanoparticles and the brain: cause for concern. J Nanosci Nanotechnol 9:4996–5007

Petty RD, Sutherland LA, Hunter EM, Cree IA (1995) Comparison of MTT and ATP-based assays for the measurement of viable cell number. J Biolumin Chemilumin 10:29–34

Reynolds BA, Weiss S (1992) Generation of neurons and astrocytes from isolated cells of the adult mammalian central nervous system. Science 255:1707–1710

Reynolds BA, Weiss S (1996) Clonal and population analyses demonstrate that an EGF-responsive mammalian embryonic CNS precursor is a stem cell. Dev Biol 175:1–13

Soderstjerna E, Johansson F, Klefbohm B, Johansson UE (2013) Gold and silver nanoparticles affect the growth characteristics of human embryonic neural precursor cells. PLOS One 8:e58211

Sung JH, Ji JH, Park JD, Yoon JU, Kim DS, Jeon KS, Song MY, Jeong J, Han BS, Han JH, Chung YH, Chang HK, Lee JH, Cho MH, Kelman BJ, Yu IJ (2009) Subchronic inhalation toxicity of silver nanoparticles. Toxicol Sci 108:452–461

Takenaka S, Karg E, Roth C, Schulz H, Ziesenis A, Heinzmann U, Schramel P, Heyder J (2001) Pulmonary and systemic distribution of inhaled ultrafine silver particles in rats. Environ Health Perspec 109:547–551

Tang JL, Xiong L, Wang S, Wang JY, Liu L, Li JG, Yuan FQ, Xi TF (2009) Distribution, translocation and accumulation of silver nanoparticles in rats. J Nanosci Nanotechnol 9:4924–4932

Tejamaya M, Romer I, Merrifield RC, Lead JR (2012) Stability of Citrate, PVP, and PEG coated silver nanoparticles in ecotoxicology media. Environ Sci Technol 46:7011–7017

Wang JY, Rahman MF, Duhart HM, Newport GD, Patterson TA, Murdock RC, Hussain SM, Schlager JJ, Ali SF (2009) Expression changes of dopaminergic system-related genes in PC12 cells induced by manganese, silver, or copper nanoparticles. Neurotoxicology 30:926–933

Zhang W, Yao Y, Sullivan N, Chen Y (2011) Modeling the primary size effects of citrate-coated silver nanoparticles on their ion release kinetics. Environ Sci Technol 45:4422–4428

Zook JM, Long SE, Cleveland D, Geronimo CLA, MacCuspie RI (2011a) Measuring silver nanoparticle dissolution in complex biological and environmental matrices using UV–visible absorbance. Anal Bioanal Chem 401:1993–2002

Zook JM, MacCuspie RI, Locasio LE, Halter MD, Elliott JT (2011b) Stable nanoparticle aggregates/agglomerates of different sizes and the effect of their size on hemolytic cytotoxicity. Nanotoxicology 5:517–530